

Omar Belguendouz<sup>1</sup>, Bendaoud Mebarek<sup>2\*</sup>, Yassine El Guerri<sup>3</sup>, Mourad Keddou<sup>4</sup>, Naima Hadjadj<sup>5,6</sup>, Youcef Djafri<sup>1</sup>

<sup>1</sup>Université Ibn Khaldoun, University of Tiaret, Laboratoire Synthèse et Catalyse, Algeria, <sup>2</sup> University of Tiaret, Laboratoire de Recherche en Intelligence Artificielle et Systèmes (LRIAS), Algeria, <sup>3</sup>Research laboratory of industrial technologies, University of Tiaret, Algeria, <sup>4</sup>Materials Technology laboratory, Faculty of Mechanical Engineering and Process Engineering, USTHB, El-Alia, Bab-Ezzouar, Algiers, Algeria, <sup>5</sup>Université de Tissemsilt, Département Sciences de la Matière, Faculté des Sciences et Technologie, Tissemsilt, Algérie, <sup>6</sup> Université des Sciences et de Technologies USTO-MB, Laboratoire d'Etudes Physique des Matériaux, El M'Naouar, Oran, Algérie

Scientific paper

ISSN 0351-9465, E-ISSN 2466-2585

<https://doi.org/10.5937/zasmat2304491B>



Zastita Materijala 64 (4)  
491 - 502 (2023)

## Simple model and integral method for simulating the growth of the borided layer FeB/Fe<sub>2</sub>B on the AISI H13 steel

### ABSTRACT

The prediction of boride layer growth kinetics requires the development of a mathematical model. In the present study, two diffusion models (a simple model and an integral method-based model) were proposed to investigate the boriding kinetics of pack-borided AISI H13 steel. These two diffusion models did not consider the effect of boride incubation times of the total boride layer (FeB + Fe<sub>2</sub>B). The diffusion coefficients of boron in the FeB and Fe<sub>2</sub>B layers were estimated using the proposed integral method-based model. Additionally, the growth rate constants were determined and the layer thickness was calculated after finding the needed parameters. The results obtained were compared to the experimental ones taken from the work of Nait Abdellah et al.[4] and a good agreement has been noticed. Finally, the mass gain has been calculated for both phases, showing that of FeB increased more compared to that of Fe<sub>2</sub>B over time.

**Keywords:** Diffusion model, simulation, boronizing, FeB, Fe<sub>2</sub>B, integral method, layer thickness

### 1. INTRODUCTION

In the industry, the need for producing harder and more wear resistant surface layer is very crucial to improve the surface properties of workpieces [1,2]. There are many processes enabling the formation of a hard layer such as; carburizing, nitriding, and boronizing. This last process is accomplished by means of diffusing boron into the steel. Boriding is then defined as a thermochemical treatment of surface hardening and can be applied to many ferrous and non-ferrous alloys as well as cermet materials [1,3]. This process is generally carried out at a temperature range of 1073 K to 1323 K for a few hours (mainly 1 to 12 h), and requires the presence of an appropriate boron source leading to the diffusion of boron atoms into the steel substrate.

A single or two-phase microstructure is then formed in the shape of a directional and superficial saw tooth microstructure [4,5].

Generally, the boride layer contains two phases (Fe<sub>2</sub>B and FeB) that depends on the parameters of the boriding process. The outer FeB phase has an orthorhombic crystal structure with a strong crystallographic anisotropy, while the inner Fe<sub>2</sub>B phase is known to have a tetragonal structure [6,7]. One of the benefits of carrying out this process is that it can produce a higher surface hardness in steel which can reach a value of 2100 HV, if compared to that of carburizing, nitriding and carbonitriding. Generally, borided steels have wear resistance similar to that of sintered carbides [2].

The properties of the produced boride layers depend on the conditions in which this process is done, such as the physical state of the boron source used, the temperature, treatment time and the type of the borided material. The boron used can be solid as in the case of paste or powder-pack boriding techniques [8,9], or liquid (with or without electrolysis)[10], or gaseous in the case of gas boriding techniques [11].

\*Corresponding author: Bendaoud Mebarek

E-mail: mebarekbendaoud@yahoo.fr

Paper received: 29.08. 2023.

Paper corrected: 22. 09. 2023.

Paper accepted: 23.09.2023.

Paper is available on the website: [www.idk.org.rs/journal](http://www.idk.org.rs/journal)

Experimentally, studying this phenomenon is difficult to achieve both technically and financially. In practice, it is experimentally difficult to measure the thickness of the boride layer. This difficulty is due to the microstructural nature of the interface (boride layer/ substrate) [12]. The AISI H13 steel exhibits outstanding properties such as a high strength, fatigue resistance and toughness with exceptional thermal softening resistance. To further improve its wear resistance, the boronizing process can be applied on this tooling steel for instance in hot forming and hot moulding processes.

The development in scientific calculations gave some good tools to simulate this process where mathematical modelling and simulation have become essential to study and predict the behaviour of boron when diffusing. Subsequently, the theoretically developed models and calculated results are then compared to the experimental results to confirm their validity. Another advantage of theoretical computational studies is the ability to study the effect of different parameters with low cost, less time and a broad range of possibilities.

In this work, we propose two diffusion models based on Fick's second law to simulate boronizing kinetics of biphasic layers (Fe<sub>2</sub>B/FeB). The subsequent calculations performed by means of these two models are aimed at predicting the

thickness of the boride layer and the boron concentration profile in each phase, for which the temperature and the processing time are needed in priori to simulate and optimize this process. To verify the validity of the proposed mathematical models, experimental data of studies about boriding in powders applied to AISI H13 steel from the literature were used, such as those that were provided by [4,13,14].

## 2. MATHEMATICAL MODELS OF DIFFUSION

The two mathematical models [15,16] which we aim at applying are based on the solution of Fick's equation, where the diffusion of boron in the iron matrix and iron boride can be described by Fick's second law:

$$\frac{\partial c_i}{\partial t} = D_i \frac{\partial^2 c_i(x,t)}{\partial x^2} \quad (1)$$

where  $C_i(x, t)$  is the concentration of boron at depth  $x$  after diffusion time  $t$ , and  $D_i$  is the diffusion coefficient which obeys a thermal activation law of the Arrhenius equation.

Fig.1 illustrates the distribution of boron concentration along the depth of the boronized layer for a given temperature and under a boron potential that allows the formation of a biphasic FeB and Fe<sub>2</sub>B layer at the material substrate.

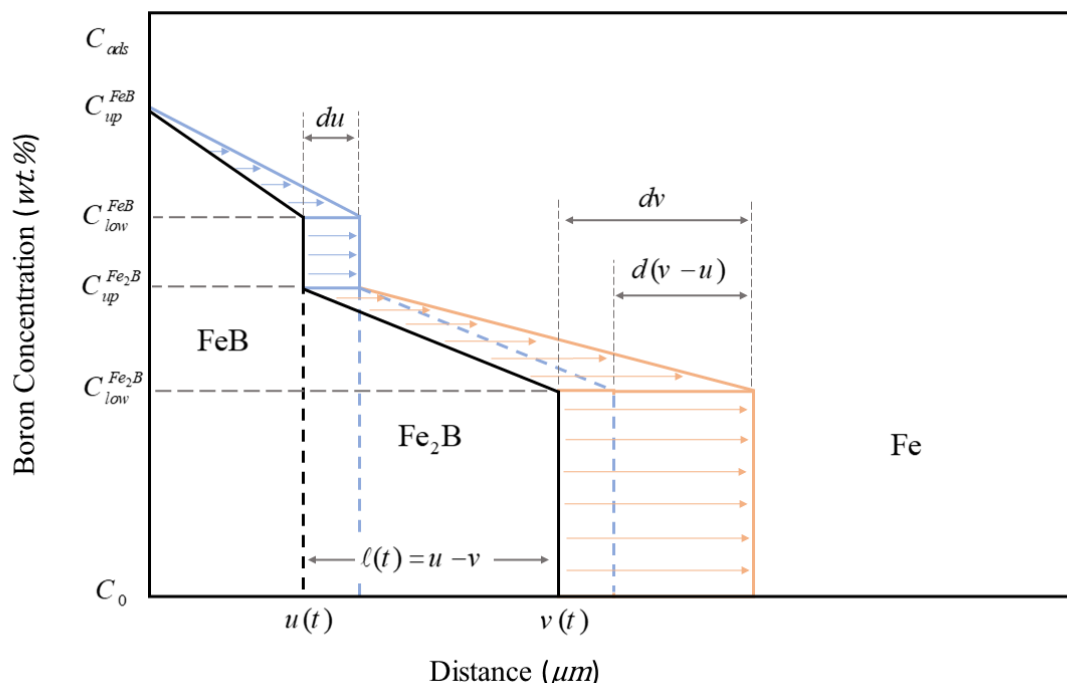


Figure 1. Schematic profile of boron concentration along the FeB and Fe<sub>2</sub>B layers [4]

Slika 1. Šematski profil koncentracije bora duž slojeva FeB i Fe<sub>2</sub>B [4].

The development of the models which we aim at applying [15,16] are based on a set of conditions

that will facilitate the calculations and provide simpler mathematical formulae without prejudicing

the integrity of the models when compared to experimental results. Thus, (1) we firstly consider only perpendicular flow of boron atoms at the surface of materials.(2) The temperature of the sample is set to be constant during the process.(3) We also assume that the concentration of boron on the surface does not change with time and temperature.(4) Iron borides are considered to develop parabolically over time.(5) The boride layer is assumed to be sufficiently thin relative to the thickness of the sample, and finally (6) the diffusion of Fe atoms may be disregarded.

These two applied models are intended to predict the thickness of the bilayer based on the following parameters: (boron surface concentration, time and temperature).

#### The simple model of the boride layer growth (FeB/Fe<sub>2</sub>B)

For the phase (Fe<sub>2</sub>B or FeB), as proposed by Kirkcaldy [17], the general solution of the equation (1) is given by the following expression:

$$C_i(x, t) = A_i + B_i \operatorname{erf}\left(\frac{x}{2\sqrt{D_i t}}\right) \quad (2)$$

where *erf* is the Gauss error function, A<sub>i</sub> and B<sub>i</sub> (with i=FeB, Fe<sub>2</sub>B or Fe) are constants to be determined according to the boundary conditions.

The interfaces (FeB/Fe<sub>2</sub>B) and (Fe<sub>2</sub>B/Fe), shift by an infinitely small distance dx, which results from the flows in and out of the surface concerned, and are expressed by the following formulae:

$$W_{FeB} \frac{k_{FeB}}{2} = \left( -\gamma_1 D_{FeB} \frac{2}{\sqrt{\pi}} \frac{1}{2\sqrt{D_{FeB}t}} e^{-\frac{x^2}{4D_{FeB}t}} - \gamma_2 D_{Fe_2B} \frac{2}{\sqrt{\pi}} \frac{1}{2\sqrt{D_{Fe_2B}t}} e^{-\frac{x^2}{4D_{Fe_2B}t}} \right) \quad (7)$$

$$W_{Fe_2B} \frac{k_{Fe_2B}}{2} + \sigma \frac{k_{FeB}}{2} = \left( -\gamma_2 D_{Fe_2B} \frac{2}{\sqrt{\pi}} \frac{1}{2\sqrt{D_{Fe_2B}t}} e^{-\frac{x^2}{4D_{Fe_2B}t}} - \gamma_3 D_{Fe} \frac{2}{\sqrt{\pi}} \frac{1}{2\sqrt{D_{Fe}t}} e^{-\frac{x^2}{4D_{Fe}t}} \right) \quad (8)$$

With

$$\gamma_1 = \frac{C_{up}^{FeB} - C_{low}^{FeB}}{\operatorname{erf}\left(\frac{k_{FeB}}{2\sqrt{D_{FeB}}}\right)}, \quad \gamma_2 = \frac{C_{low}^{FeB}}{\operatorname{erfc}\left(\frac{k_{Fe_2B}}{2\sqrt{D_{Fe_2B}}}\right)}, \quad \gamma_3 = \frac{C_{low}^{Fe_2B}}{\operatorname{erfc}\left(\frac{k_{Fe_2B}}{2\sqrt{D_{Fe}}}\right)}$$

After solving these two equations, the solutions ( $k_{Fe_2B}$  and  $k_{FeB}$ ) are used to calculate the thicknesses of the boride layers (*u* and *v*) and also to determine the change in boron concentration with respect to the depth.

#### The diffusion model based on the integral method

This model considers the growth of Fe<sub>2</sub>B and FeB layers at the steel surface, the distribution of boron concentration along these two layers is described by Fick's second law given by equation

$$W_{FeB} \frac{du}{dt} = \left( -D_{FeB} \frac{\partial C_{FeB}}{\partial x} + D_{Fe_2B} \frac{\partial C_{Fe_2B}}{\partial x} \right)_{x=u} \quad (3)$$

$$W_{Fe_2B} \frac{dv}{dt} + \sigma \frac{du}{dt} = \left( -D_{Fe_2B} \frac{\partial C_{Fe_2B}}{\partial x} + D_{Fe} \frac{\partial C_{Fe}}{\partial x} \right)_{x=v} \quad (4)$$

$$\text{With } W_{FeB} = \frac{1}{2} (C_{up}^{FeB} - C_{low}^{FeB}) + (C_{up}^{Fe_2B} - C_{low}^{Fe_2B}),$$

$$W_{Fe_2B} = \frac{1}{2} (C_{up}^{Fe_2B} - C_{low}^{Fe_2B}) + (C_{low}^{Fe_2B} - C_0),$$

$$\sigma = \frac{1}{2} (C_{up}^{Fe_2B} - C_{low}^{Fe_2B})$$

The variables *u* and *v* are respectively the interfaces' positions of (FeB/Fe<sub>2</sub>B) and (Fe/Fe<sub>2</sub>B) interfaces. The two terms *u* and *v* are respectively the FeB layer thickness and the total thickness of (FeB+Fe<sub>2</sub>B).

$$u = k_{FeB} \sqrt{t} \quad (5)$$

and

$$v = k_{Fe_2B} \sqrt{t} \quad (6)$$

The two terms  $k_{Fe_2B}$  and  $k_{FeB}$  are the parabolic growth constant at the two interfaces, respectively. Equations (7) and (8) can be obtained from equations (3) and (4), by considering the time derivatives of equations (5) and (6) as well as the derivation of equation (2) with respect of the diffusion distance at the two positions  $x=u$  and  $x=v$  :

(1).  $C_{ads}$  is given as the amount of boron adsorbed on the material surface.

$C_{up}^{FeB}$  and  $C_{low}^{FeB}$  (= 16.23 % in B-weight) represent the values of the upper and lower boron levels in the FeB layer, while  $C_{up}^{Fe_2B}$  and  $C_{low}^{Fe_2B}$  (= 8.83% in B-weight) are the values of the upper and lower boron levels in the Fe<sub>2</sub>B layer.  $C_0$  is the limit of boron solubility in the substrate for which we set a value of  $35 \times 10^{-4}$ % in weight of boron. *u* and *v* are respectively the thicknesses of the FeB and (FeB

+Fe<sub>2</sub>B) layers, which vary with the processing time according to Equations (5) and (6). In the integral method, the variation of boron concentration with respect to time and the depth (distance) of diffusion in each boride layer is not linear and satisfies the second Fick's law given by equation (1). The mathematical expressions of boron concentrations in each phase are essential to apply this approach, where they are considered to have a parabolic form as suggested by the Goodman method [18,19]. Therefore, boron concentrations along the FeB (0 ≤ x ≤ u) and Fe<sub>2</sub>B (u ≤ x ≤ v) layers are given respectively by the equations (9) and (10) as follows:

$$C_{FeB}(x, t) = C_{low}^{FeB} + a_1(t)(u(t) - x) + b_1(t)(u(t) - x)^2 \tag{9}$$

$$C_{Fe_2B}(x, t) = C_{low}^{Fe_2B} + a_2(t)(v(t) - x) + b_2(t)(v(t) - x)^2 \tag{10}$$

The parameters a<sub>1</sub>(t), b<sub>1</sub>(t), a<sub>2</sub>(t), b<sub>2</sub>(t), u(t) and v(t) must meet the boundary conditions. Thus, when applying these conditions at the steel surface and at the (FeB/ Fe<sub>2</sub>B) interface, we get respectively, equations (11) and (12):

$$a_1(t)u(t) + b_1(t)u^2(t) = (C_{up}^{FeB} - C_{low}^{FeB}) \tag{11}$$

$$a_2(t)[v(t) - u(t)] + b_1(t)[v(t) - u(t)]^2 = (C_{up}^{Fe_2B} - C_{low}^{Fe_2B}) \tag{12}$$

by integrating Fick's second law between 0 and u for the FeB phase, and between u and v for the Fe<sub>2</sub>B phase, and after applying the Leibniz rule, we arrive at the following ordinary differential equations (13):

$$\frac{d}{dt} \left[ \frac{u^2(t)}{2} a_1(t) + \frac{u^3(t)}{3} b_1(t) \right] = 2D_B^{FeB} b_1(t)u(t) \tag{13}$$

$$2 w_{12} \frac{dv(t)}{dt} + \frac{[v(t)-u(t)]^2}{2} \frac{da_2(t)}{dt} + \frac{[v(t)-u(t)]^3}{3} \frac{db_2(t)}{dt} = 2D_B^{Fe_2B} b_2(t)[v(t) - u(t)] \tag{14}$$

The two algebraic constraints applied on this diffusion problem can be derived from the continuity equations at the two considered interfaces as follows:

$$2 w_1 b_1(t) D_B^{FeB} = D_B^{FeB} a_1^2(t) - D_B^{Fe_2B} a_1(t)(a_2(t) + 2b_2(t)[v(t) - u(t)]) \tag{15}$$

with

$$w_1 = \left[ \frac{(C_{up}^{FeB} + C_{low}^{FeB})}{2} - C_{up}^{Fe_2B} \right]$$

$$2 w_{12} b_1(t) D_B^{FeB} a_2(t) + 2 w_2 b_2(t) D_B^{Fe_2B} a_1(t) = D_B^{Fe_2B} a_2^2(t) a_1(t) \tag{16}$$

With

$$w_2 = \left[ \frac{(C_{up}^{Fe_2B} + C_{low}^{Fe_2B})}{2} - C_0 \right]$$

$$\text{and } w_{12} = \frac{(C_{up}^{Fe_2B} - C_{low}^{Fe_2B})}{2}$$

Equations (11) to (16) form a differential-algebraic system of equations (DAE) whose unknowns are a<sub>1</sub>(t), b<sub>1</sub>(t), a<sub>2</sub>(t), b<sub>2</sub>(t), u(t) and v(t), must comply with the given algebraic constraints. This system of DAE can therefore be solved analytically, after using appropriate changes of variables [15]. Thus, the expression of boron diffusion coefficients in the FeB and Fe<sub>2</sub>B phases are calculated by equations (17) and (18):

$$D_B^{FeB} = (k_{FeB})^2 \left[ \frac{(C_{up}^{FeB} - C_{low}^{FeB})}{8\beta_1} - \frac{1}{24} \right]$$

$$\text{for } \beta_1 < 3 (C_{up}^{FeB} - C_{low}^{FeB}) \tag{17}$$

$$D_B^{Fe_2B} = \frac{k_{Fe_2B}(k_{Fe_2B} - k_{FeB})(C_{up}^{Fe_2B} - C_{low}^{Fe_2B})}{4\beta_2} - (k_{Fe_2B} - k_{FeB})^2 \left[ \frac{(C_{up}^{Fe_2B} - C_{low}^{Fe_2B})}{8\beta_1} - \frac{1}{24} \right] \tag{18}$$

After determining the diffusivity of boron in each phase, the thickness u(t) and v(t) of the boride layer can be calculated for a given time and temperature.

### 3. EXPERIMENTAL PROCEDURE

The process of boriding of AISI H13 steel was carried out with the powder technique using (90 wt.% B<sub>4</sub>C and 10 wt.% NaBF<sub>4</sub>), at three temperatures, 1073 K, 1173 K and 1273 K, each

for 2, 4 and 6 h [4]. The boronizing process was realized in an electrical resistance furnace. The chemical composition of the steel used for boriding is given in Table 1.

Table 1. The chemical composition of the steel used (% mass) [4]

Tabela 1. Hemijski sastav korišćenog čelika (% mase) [4]

| Elements (wt%) | C    | Mn   | Si | V   | Mo   | Cr   |
|----------------|------|------|----|-----|------|------|
|                | 0.45 | 0.35 | 1  | 1.1 | 1.65 | 5.25 |

The samples are borided by varying the processing time and temperature, the temperature range from 1073 K to 1273 K within a duration of 2 to 6 h. The thicknesses of the resulting boride layers (FeB and Fe<sub>2</sub>B) were measured using the method proposed by Yu et al. [20].

When boriding with powders, the parts are placed in crucible filled with powder and put into the resistance furnace. This process is most advantageous because of its easy handling, the ability to change the composition of the powder, and the very small equipment.

Just before processing, all samples underwent a surface pre-treatment (preparation) with abrasive elements to eliminate any contamination that may interfere with boron diffusion during the experiments.

To measure the thickness of the boride layer, a method was proposed by Brakman et al. [21], where only FeB or Fe<sub>2</sub>B needles which penetrates most deeply are selected as an indication of layer thickness. To ensure the accuracy of the layer thickness measurements, an average of 10 measurements were taken on different locations of the cross sections of the borided samples [20]. Another procedure was proposed by Chatterjee-Fisher [22], where the average finger height is used to define the layer thickness. However, such methods do not consider the fingers' width. In order to take both the finger height and width into account, Yu et al. [20] proposed that in order to calculate the boride layer thickness (d), the boride layer area (A) is used which includes the area of all fingers, and divides it by the boride layer length (L), as it is stated in the equation (19):

$$d = \frac{A}{L} \quad (19)$$

the area of the borided layer is calculated using an image-processing program developed by Yu et al. [20].

Table 2 shows the experimental values obtained by Nait Abdellah et al. [4] concerning the experimental values of parabolic growth constants at the (FeB/Fe<sub>2</sub>B) and (Fe<sub>2</sub>B/substrate) interfaces for increasing temperatures that range from 1173

to 1273 K. These values were extracted by fitting the experimental data using equations (12) and (13) without including the boride incubation times [4].

Table 2. Experimental data of  $k_{Fe_2B}$  and  $k_{FeB}$  [4]

Tabela 2. Eksperimentalni podaci za  $k_{Fe_2B}$  i  $k_{FeB}$  [4]

| Temperature | Growth rate constant ( $\mu\text{m/s} \cdot 0.5$ ) |             |
|-------------|--|-------------|
|             | $k_{FeB}$  | $k_{Fe_2B}$ |
| 1173        | 0.1851   | 0.3437      |
| 1223        | 0.2721   | 0.5121      |
| 1273        | 0.4833   | 0.8853      |

#### 4. SIMULATION RESULTS AND DISCUSSION

##### Estimation of boron activation energy

The diffusion coefficient can be related to the processing time and thickness of the boride layer by Arrhenius expression. To estimate the boron activation energy, we must have a minimum of three processing temperatures for three treatment times [4]. Based on the experimental data taken from Nait Abdellah et al. [4], we can estimate the activation energy of boron diffusion in the AISI H13 steel by using the equation (20):

$$u^2 = D_0 t \cdot \exp\left(-\frac{Q_d}{RT}\right) \quad (20)$$

The variable  $u$  represents the thickness of the boride layer in ( $\mu\text{m}$ ),  $D_0$  is the boron diffusion coefficient ( $\mu\text{m}^2/\text{s}$ ),  $t$  is the boriding time,  $Q_d$  is the value of the activation energy measured in Joule/mol,  $R$  is the gas constant and  $T$  is the temperature in Kelvin.

It is easy to estimate the value of the activation energy  $Q_d$  using Arrhenius's Law in a linear form of equation (20), where  $Q_d$  can be easily deduced from the slope of the straight line obtained in (kJ/mol). Therefore, the boron diffusion coefficients are calculated with this method as follows [23]:

$$D_{FeB} = 7.61 \times 10^{-2} \exp\left(-\frac{236.43 \text{ kJ mol}^{-1}}{RT}\right) (\text{m}^2 \text{s}^{-1}) \quad (21)$$

$$D_{Fe_2B} = 3.22 \times 10^{-2} \exp\left(-\frac{233.04 \text{ kJ mol}^{-1}}{RT}\right) (\text{m}^2 \text{s}^{-1}) \quad (22)$$

##### Calculation of the boron diffusion coefficient by the Integral method

In order to improve the predictability of the model, it is necessary to find precise measurements of the diffusion coefficient of boron in each phase. Using the following equations provided by the integral method, we can calculate the boron diffusion coefficient in each phase with ( $k_{Fe_2B} = k$ ,  $k_{FeB} = k'$ ) by using Equations (17) and

(18). In our calculations, the boron concentration at the surface level is  $C_{up}^{FeB} = 16.40$  wt.%B and at the FeB/Fe<sub>2</sub>B interface is given as:  $C_{low}^{FeB} = 16.23$  wt.%B, both representing the maximum and minimum boron contents in FeB respectively. The values  $C_{up}^{Fe2B} = 9$  wt.%B and

$C_{low}^{Fe2B} = 8.83$  wt.%B stand for the maximum and minimum boron contents in Fe<sub>2</sub>B and at the (Fe<sub>2</sub>B/Fe) interface,  $C_0 = 35 \times 10^{-4}$  wt.% B

From the equations (17) and (18), the diffusion coefficients for each temperature are calculated and the results are depicted in Table 3.

Table 3. Calculated diffusion coefficients for varying temperatures for both phases

Tabela 3. Izračunati koeficijenti difuzije za različite temperature za obe faze

| Temperature (K) | $D_B^{FeB}$             |                         | $D_B^{Fe_2B}$          |                        |
|-----------------|-------------------------|-------------------------|------------------------|------------------------|
|                 | Experimental [4]        | Integral method         | Experimental [4]       | Integral method        |
| 1173            | $2.41 \times 10^{-12}$  | $2.252 \times 10^{-12}$ | $1.42 \times 10^{-12}$ | $1.35 \times 10^{-12}$ |
| 1223            | $5.26 \times 10^{-12}$  | $6.07 \times 10^{-12}$  | $3.22 \times 10^{-12}$ | $3.58 \times 10^{-12}$ |
| 1273            | $16.28 \times 10^{-12}$ | $15.12 \times 10^{-12}$ | $9.32 \times 10^{-12}$ | $8.82 \times 10^{-12}$ |

Table 3 shows that the theoretical values of diffusion coefficients obtained from the integral method agree to a great precision with those derived experimentally from the parabolic law reported in the work of Nait Abdellah et al. [4]. This agreement is shown to hold for all three temperatures.

*Simulation of the kinetics of the boriding process by the simple diffusion model*

In order to run numerical simulations of boriding kinetics using the proposed model, the parameters needed are the temperature, boriding time and diffusivity of boron in each phase, as well as the concentration of boron in each boride phase.

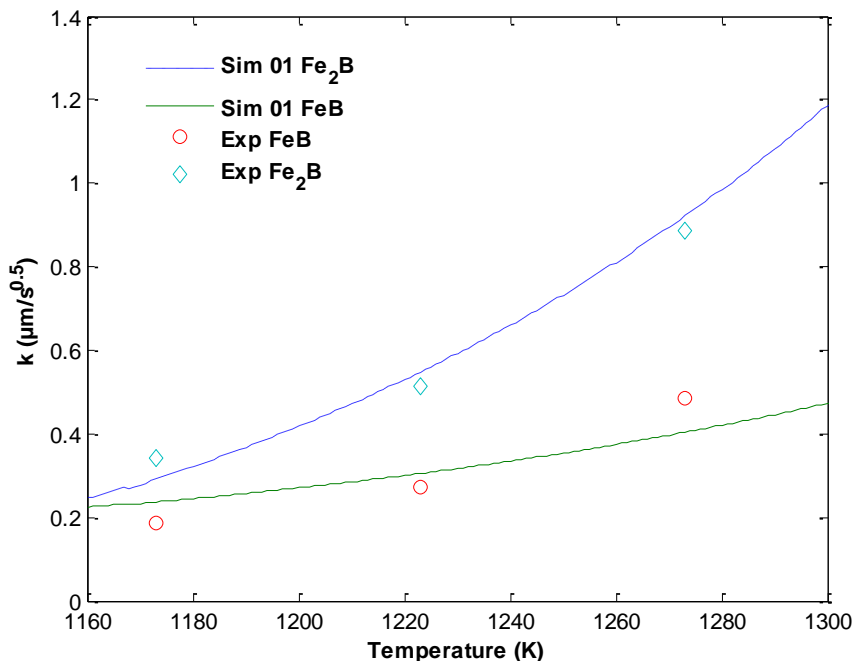


Figure 2. Temperature-based variation of the growth rate constants at the first and second interfaces

Slika 2. Varijacija konstanti brzine rasta na prvom i drugom interfejsu na osnovu temperature

Whereas the kinetic data and boron activation energies for iron substrate were taken from [12]. Boron diffusion coefficients in the  $\alpha$ -Fe and  $\gamma$ -Fe phases were found in [5,12]. Boron diffusion coefficients in iron borides ( $m^2/s$ ) are given in the previous section.

Figure 2 shows the increase in the temperature-related growth rate constant at the first and second interfaces, where there is a good agreement between the simulation results and experimental data. It is seen that the growth rate constants change exponentially. Additionally, the

growth rate constant for Fe<sub>2</sub>B is shown to increase more rapidly with respect to the process temperature, in contrast to that of FeB which increases slowly. This is also demonstrated via the noticed amount of change as the temperature increases, where the variation in the growth rate constant at the second interface reached a value of 1.2 μm/s<sup>0.5</sup> at 1300 K which is a threefold increase compared to 0.5 μm/s<sup>0.5</sup> for FeB.

*Simulation of the boriding process kinetics by the integral method-based model*

To search for the simulated values of growth rate constants, numerical solutions of the obtained non-linear equations (23) and (24) are then required. Therefore, the thickness of each iron boride layer can be easily predicted once the growth rate constants are determined.

$$k_{FeB} = \sqrt{\frac{D_B^{FeB}}{\frac{C_{up}^{FeB} - C_{low}^{FeB}}{8\beta_1} - \frac{1}{24}}} \tag{23}$$

$$D_B^{Fe_2B} = \frac{k(k_{Fe_2B} - k_{FeB})(C_{up}^{Fe_2B} - C_{low}^{Fe_2B})}{4\beta_2} - (k_{Fe_2B} - k_{FeB})^2 \left[ \frac{(C_{up}^{Fe_2B} - C_{low}^{Fe_2B})}{8\beta_2} + \frac{1}{24} \right] \tag{24}$$

with

$$(k_{Fe_2B} = k, k_{FeB} = k')$$

The obtained values of the growth rate constants are given in Table 4.

Table 4. Comparison between the predicted growth rate constants and the experimental values

Tabela 4. Poređenje između predviđenih konstanti stope rasta i eksperimentalnih vrednosti

| Temperature (K)                  | Growth rate Constants $k$ (μm/s <sup>0.5</sup> ) |                        |                           |                   |                        |                           |
|----------------------------------|--|------------------------|---------------------------|-------------------|------------------------|---------------------------|
|                                  | FeB  |                        |                           | Fe <sub>2</sub> B |                        |                           |
|                                  | Exp.[4]  | Sim 01<br>Simple model | Sim 02<br>Integral method | Exp.[4]           | Sim 01<br>Simple model | Sim 02<br>Integral method |
| 1173                             | 0.1851   | 0.236                  | 0.1733                    | 0.3437            | 0.2909                 | 0.3494                    |
| 1223                             | 0.2721   | 0.3049                 | 0.2844                    | 0.5121            | 0.5540                 | 0.5694                    |
| 1273                             | 0.4833   | 0.4060                 | 0.4491                    | 0.8853            | 0.9211                 | 0.8931                    |
| Average error of simulation (μm) |  | 0.0537                 | 0.0194                    |                   | 0.0435                 | 0.0236                    |
| Error of simulation (%)          |  | 5.37%                  | 1.9%                      |                   | 4.35%                  | 2.36%                     |

From Table 4, we notice that both models lead to results which are consistent with the experimental data taken from the work of Nait Abdellah et al. [4]. The integral method is clearly shown to have results more compatible with experiments, with a decreasing error by nearly a half when compared to the simulation error of the simple model. This confirms the validity and precision of the integral method-based model implemented in this work.

Consequently, using the model we have proposed, we can thus calculate the thickness of the boride layer in each phase. This can be done after calculating all the parameters involved and needed. Therefore, the values of  $\alpha_1$ ,  $\beta_1$ ,  $\alpha_2$  and  $\beta_2$  constants are calculated using the procedure given in the reference work [15] and depicted in Tab.5, where the calculations were made for a concentration of  $C_{up} = 16.40$  wt.% B and temperatures that range between 1173 K and 1273 K.

Table 5. The calculated value of  $\alpha_1$ ,  $\beta_1$ ,  $\alpha_2$  and  $\beta_2$  constants

Tabela 5. Izračunata vrednost konstanti  $\alpha_1$ ,  $\beta_1$ ,  $\alpha_2$  i  $\beta_2$

| Temperature (K) | $\alpha_1, \beta_1, \alpha_2$ and $\beta_2$ Constants |           |                   |           |
|-----------------|---|-----------|-------------------|-----------|
|                 | FeB   |           | Fe <sub>2</sub> B |           |
|                 | $\alpha_1$  | $\beta_1$ | $\alpha_2$        | $\beta_2$ |
| 1173            | 0.1661  | 0.0039    | 0.2317            | 0.0617    |
| 1223            |   |           |                   |           |
| 1273            |   |           |                   |           |

From the values of the constants  $\alpha_1, \beta_1, \alpha_2$  and  $\beta_2$ , we calculate the parameters  $a_1, b_1, a_2$  and  $b_2$  for different temperatures and at different times that

range between 1 and 10 h. The results of these calculations are shown in Figure 3.

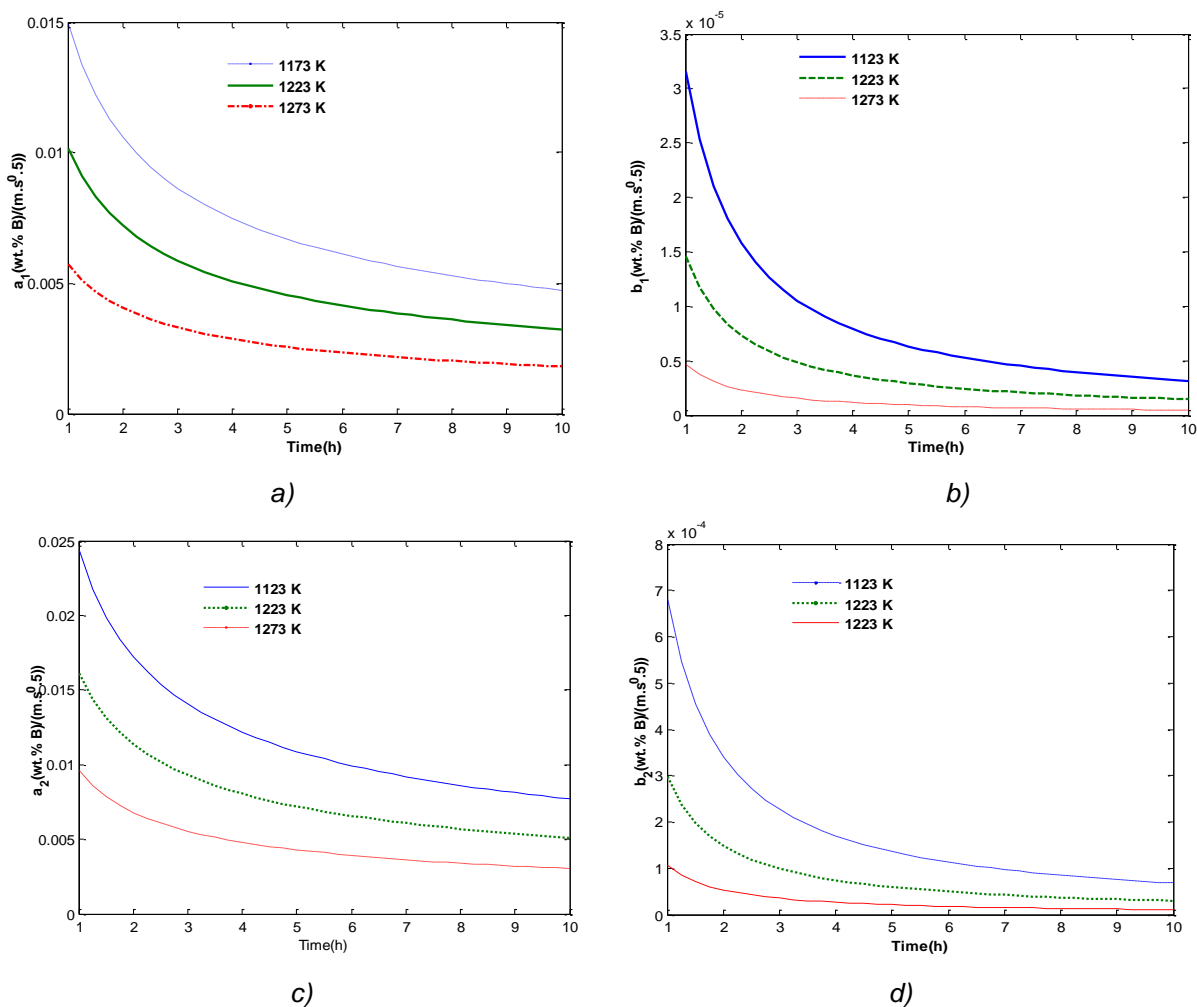


Figure 3. Values of  $a_1$  (a),  $b_1$  (b),  $a_2$  (c),  $b_2$  (d) as a function of time for different temperatures  
 Slika 3. Vrednosti  $a_1$  (a),  $b_1$  (b),  $a_2$  (c),  $b_2$  (d) kao funkcija vremena za različite temperature

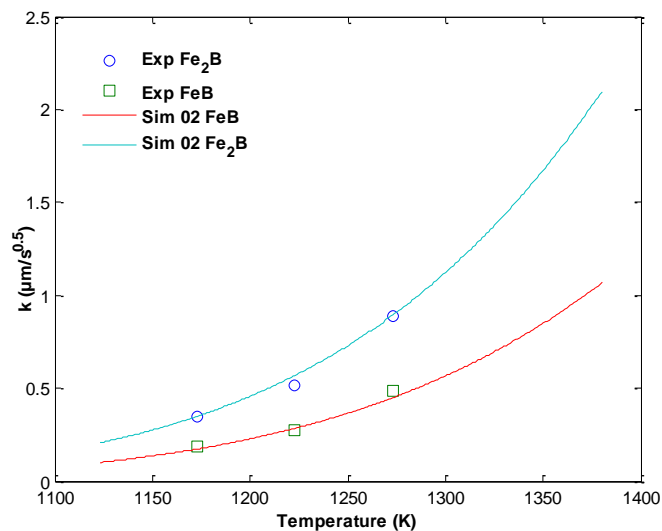


Figure 4. Variation of the growth rate constants of  $\text{FeB}$  and  $\text{Fe}_2\text{B}$  as a function of temperature calculated by the integral method and compared to the experimental results from [4]

Slika 4. Varijacija konstanti brzine rasta  $\text{FeB}$  i  $\text{Fe}_2\text{B}$  u funkciji temperature izračunata integralnom metodom i upoređena sa eksperimentalnim rezultatima iz [4]



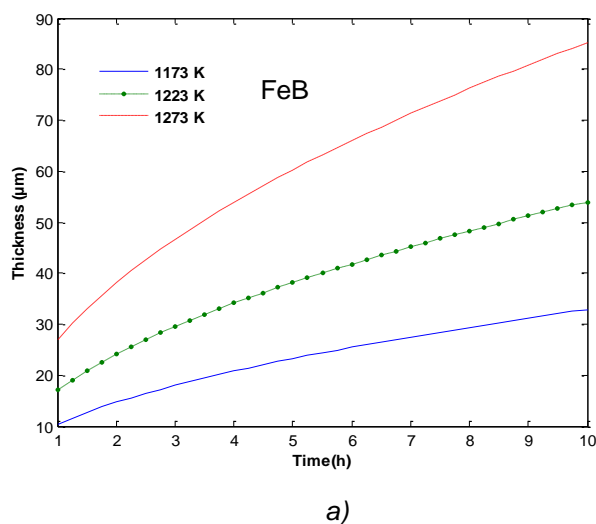
Figure 3 shows that the value of each parameter decreases exponentially with increasing time. It is also evident that the increase in temperature leads also to a decrease in the value of each parameter at any given time.

Figure 4 shows that for both phases FeB and Fe<sub>2</sub>B, the growth rate constant increases exponentially with respect to the increasing temperature. The theoretical results obtained from the simulation are shown to have a good coincidence with the experimental data [4].

The estimation of the values of  $a_1$ ,  $b_1$ ,  $a_2$  and  $b_2$  parameters, according to the procedure given in the reference work [15], allow us to calculate theoretically the iron boride layer thickness using the integral method.

The boride layers thicknesses are estimated by using equations (25) and (26):

$$u(t) = \alpha_1 \cdot \frac{1}{a_1(t)} \quad (25)$$



$$v(t) = \frac{\alpha_2}{a_2(t)} + u(t) \quad (26)$$

Table 6 shows the results obtained from the simulation compared to the experimental ones taken from Nait Abdellah et al.[4].

Table 6. Comparison between the experimental layer thicknesses of (FeB+ Fe<sub>2</sub>B) and the simulated values using the integral method

Tabela 6. Poređenje između eksperimentalnih debljina sloja (FeB+ Fe<sub>2</sub>B) i simuliranih vrednosti primenom integralne metode

|                 | Layer thickness (μm)     |                           |
|-----------------|--------------------------|---------------------------|
|                 | Exp [4]                  | Sim                       |
| Temperature (K) | (FeB+ Fe <sub>2</sub> B) | (FeB + Fe <sub>2</sub> B) |
| 1198 (for 1 h)  | 26±2.9                   | 26.89                     |
| 1198 (for 3 h)  | 44±3.5                   | 46.58                     |

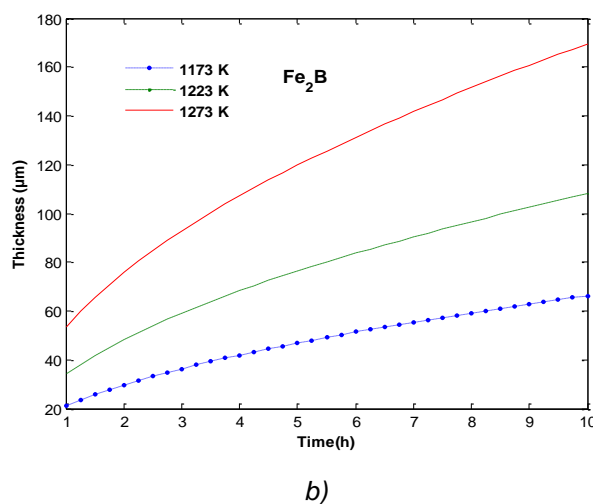


Figure 5. Evolution of the layer thickness: (a) the FeB boride layer and (b) the Fe<sub>2</sub>B layer with respect to time for three different temperatures

Slika 5. Evolucija debljine sloja: (a) sloj FeB borida i (b) sloj Fe<sub>2</sub>B u odnosu na vreme za tri različite temperature

Figure 5 demonstrates the evolution of thicknesses of FeB and Fe<sub>2</sub>B layers with respect to time which ranges from 1 to 10 h. The results are also given for three different temperatures in the range of 1173 to 1273 K

From Figure 5, the thicknesses of both Fe<sub>2</sub>B and FeB layers are shown to increase parabolically with respect to increasing time. The process temperature is also noticed to have a strong effect

on the thickness of each layer, where higher temperatures lead to thicker layers, and a more rapid increase in the layer growth. For all temperatures, the Fe<sub>2</sub>B layer shows a twofold increase when compared to FeB, where the maximum of Fe<sub>2</sub>B layer thickness is shown to go near 180 μm at 1273K, in contrast to 90 μm for FeB at the same temperature (figure 6).

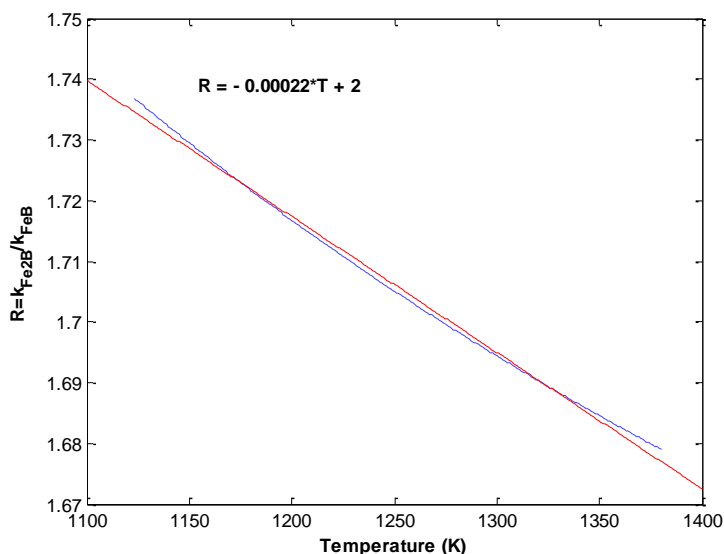


Figure 6. The ratio of the growth rate constants for Fe<sub>2</sub>B and FeB layers

Slika 6. Odnos konstanti brzine rasta za slojeve Fe<sub>2</sub>B i FeB

Mass gain

The mass gain for the FeB and Fe<sub>2</sub>B phases per unit surface can be calculated using the equations (27) and (28):

$$G(t)_{FeB} = \frac{2\rho(C_B^{S/FeB} - C_B^{FeB/Fe_2B})}{\text{erf}\left(\frac{k_{FeB}}{2\sqrt{D_B^{Fe_2B}t}}\right)} \sqrt{\frac{D_B^{Fe_2B}t}{\pi}} \quad (27)$$

In the same way, the masse gain generated by the formation of Fe<sub>2</sub>B phase can also be derived as follows:

$$G(t)_{Fe_2B} = \frac{2\rho(C_B^{Fe_2B/Fe} - C_B^{Fe_2B/FeB})}{\left[\text{erf}\left(\frac{k_{FeB}}{2\sqrt{D_B^{Fe_2B}t}}\right) - \text{erf}\left(\frac{k_{Fe_2B}}{2\sqrt{D_B^{Fe_2B}t}}\right)\right]} \sqrt{\frac{D_B^{Fe_2B}t}{\pi}} \quad (28)$$

We consider that the Fe<sub>2</sub>B and FeB layer form instantly.  $G_{FeB}(t)$  and  $G_{Fe_2B}(t)$  are the mass gains per unit surface area (g/cm<sup>2</sup>) for FeB and Fe<sub>2</sub>B,  $\rho_{Fe_2B} = 7.336$  g/cm<sup>3</sup> is the specific volume of Fe<sub>2</sub>B layer and  $\rho = 7.86$  g/cm<sup>3</sup> represents the specific volume of iron,  $k$  and  $k'$  are the growth rate constants, and  $t$  is the time duration.

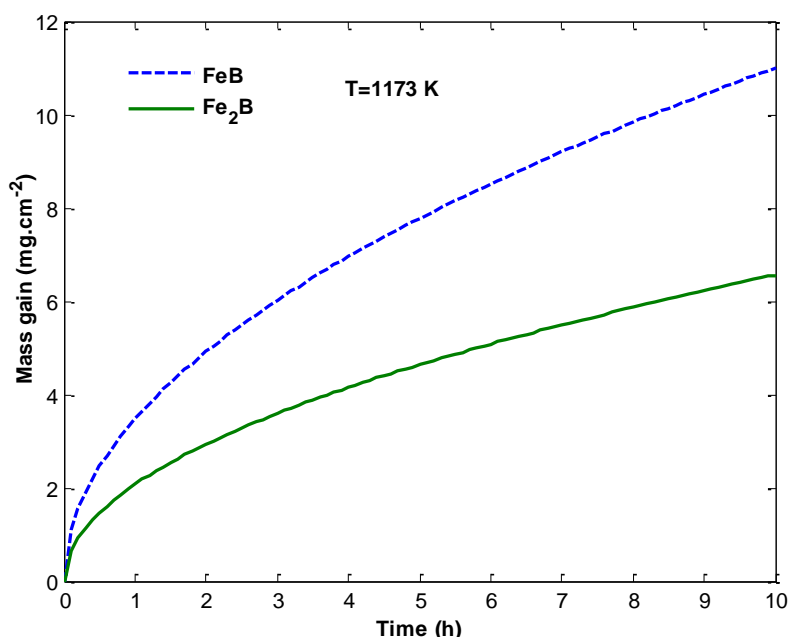


Figure 7. Mass gain values estimated in the FeB and Fe<sub>2</sub>B layers for 1173 K

Slika 7. Vrednosti povećanja mase procenjene u slojevima FeB i Fe<sub>2</sub>B za 1173 K

Figure 7 presents the time dependence of the calculated mass gains of FeB and Fe<sub>2</sub>B layers at a temperature of 1173 K, where it is shown that the mass gains for both phases increase as the time increases. The mass gain of the FeB phase is noticed to be greater than that of the Fe<sub>2</sub>B phase, and the difference between the two phases in mass gain increases with respect to increasing time.

## 5. CONCLUSION

Modelling of boron diffusion in the boriding process is crucial to theoretically study the effect of different parameters, and predict the behaviour of this phenomenon, which is important to develop and apply this method technologically. The aim of this work was to simulate the kinetics of the thermochemical boriding of AISI H13 steel using a diffusion model based on the solution of the Fick's equation in the range of temperatures from 1173 to 1323 K.

In this work, we proposed two models to study the diffusion of boron in the AISI H13 steel. The first one is a simple conventionally derived model, and the second one is an integral method-based model. Through these two models, we were able to predict the growth rate constants for Fe<sub>2</sub>B and FeB phases. Their values increased exponentially with respect to the process temperature.

The layer thickness was found to increase parabolically with time. High temperatures were noticed to lead to thicker layers, and resulted in a more rapid increase of the layer growth. The Fe<sub>2</sub>B layer thickness showed a twofold increase when compared to that of FeB. When compared to the experimental data taken from the work of Nait Abdellah et al.[4], the obtained results were shown to be, to a higher degree of certitude, in agreement with experiments, especially the integral method. This method has an error less by nearly half when compared to the simulation error using the simple model. This outcome validates the accuracy of the refined integral method approach. Finally, the mass gain was calculated for both boride phases and showed an increase with time at 1173 K. As a main result, the calculated mass gain for the FeB phase was important compared to that of the Fe<sub>2</sub>B phase.

## 6. REFERENCES

- [1] M.Kulka (2019) Current Trends in Boriding. Techniques, Engineering Materials book series, Springer International Publishing. <https://doi.org/10.1007/978-3-030-06782-3>
- [2] I.E.Campos-Silva, G.A.Rodriguez-Castro (2015) Boriding to improve the mechanical properties and corrosion resistance of steels, Thermochemical surface engineering of steels, p.651-702. <https://doi.org/10.1533/9780857096524.5.651>
- [3] H.Kunst, O.Schaaber (1967) The surface boriding of steel. Pt. 2. Growth mechanism and structure of intermediate and diffusion layers. *Harterei Tech Mitt*, 22(1), 1-25.
- [4] Z.Nait Abdellah et al. (2021) Experimental evaluation and modelling of the boronizing kinetics of AISI H13 hot work tool steel. *Materials Testing*, 63(12),1136-1141. <https://doi.org/10.1515/mt-2021-0056>
- [5] I.Campos-Silva et al. (2012) Kinetics and boron diffusion in the FeB/Fe<sub>2</sub>B layers formed at the surface of borided high-alloy steel. *Journal of materials engineering and performance*, 21(8),1714-1723. <https://doi.org/10.1007/s11665-011-0088-9>
- [6] J.Zhong et al. (2019) Mechanism of texture formation in iron boride coatings on low-carbon steel. *Metallurgical and Materials Transactions A*, 50(1), 58-62. <https://doi.org/10.1007/s11661-018-5002-8>
- [7] T.Turkoglu, I.Ay (2021) Investigation of mechanical, kinetic and corrosion properties of borided AISI 304, AISI 420 and AISI 430. *Surface Engineering*, 37(8), 1020-1031. <https://doi.org/10.1080/02670844.2021.1884332>
- [8] I.Campos-Silva et al. (2021) Pulsed-DC powder-pack boriding: Growth kinetics of boride layers on an AISI 316 L stainless steel and Inconel 718 superalloy. *Surface and Coatings Technology*, 421, 127404. <https://doi.org/10.1016/j.surfcoat.2021.127404>
- [9] K.Anthymidis et al. (2020) Production and Characterization of Boride Coatings on Steels. in *Key Engineering Materials*. Trans Tech Publ.
- [10] N.T.H.Pham et al. (2021) A Study of SiC/Borax Liquid Boride Layer on AISI H13 Hot Work Tool Steel. *International Journal of Applied Engineering & Technology*, 3(1), 23-28.
- [11] M.Kulka et al. (2013) Simulation of the growth kinetics of boride layers formed on Fe during gas boriding in H<sub>2</sub>-BCl<sub>3</sub> atmosphere. *Journal of Solid State Chemistry*, 199, 196-203. <https://doi.org/10.1016/j.jssc.2012.12.029>
- [12] B.Mebarek, SA.Bouaziz, A.Zanoun (2012) Modèle de simulation pour l'étude de la boruration thermochimique de l'acier inoxydable « AISI 316 » (X5CrNiMo17-12-2), *Matériaux & Techniques*, 100, 167-175. <https://doi.org/10.1051/mattech/2012009>
- [13] A.Günen et al. (2020) Properties and corrosion resistance of AISI H13 hot-work tool steel with borided B<sub>4</sub>C powders. *Metals and Materials International*, 26(9), 1329-1340. [doi:10.1007/s12540-019-00421-0](https://doi.org/10.1007/s12540-019-00421-0)
- [14] K.Genel (2006) Boriding kinetics of H13 steel. *Vacuum*, 80, 451-457. [doi:10.1016/j.vacuum.2005.07.013](https://doi.org/10.1016/j.vacuum.2005.07.013)
- [15] M.Keddam, M.Kulka (2018) Simulation of the growth kinetics of FeB and Fe<sub>2</sub>B layers on AISI D2 steel by the integral method. *Physics of Metals and Metallography*, 119(9), 842-851. [doi:10.1134/S0031918X18090065](https://doi.org/10.1134/S0031918X18090065)

- [16] S.Mansour et al. (2022) Prediction models for the kinetics of iron boride layers on AISI 316L steel. *Koroze a ochrana materialu*, 66(1), 40-49. <https://doi.org/10.2478/kom-2022-0007>
- [17] JS.Irkaldy, D.J.Young (1987) Diffusion in the condensed state. The Institute of Metals, 1 Carlton House Terrace, London.
- [18] T.Roodman (1964) Application of integral methods to transient nonlinear heat transfer, in *Advances in heat transfer*, Elsevier, p.51-122. [https://doi.org/10.1016/S0065-2717\(08\)70097-2](https://doi.org/10.1016/S0065-2717(08)70097-2)
- [19] A.Contla-Pacheco et al. (2021) Application of the Heat Balance Integral Method to the growth kinetics of nickel boride layers on an Inconel 718 superalloy. *Surface and Coatings Technology*, 420, 127355. <https://doi.org/10.1016/j.surfcoat.2021.127355>
- [20] L.Yu et al. (2005) FeB/Fe<sub>2</sub>B phase transformation during SPS pack-boriding: Boride layer growth kinetics. *Acta Materialia*, 53(8), 2361-2368. <https://doi.org/10.1016/j.actamat.2005.01.043>
- [21] C.Brakman et al. (1989) Boriding of Fe and Fe–C, Fe–Cr, and Fe–Ni alloys; boride-layer growth kinetics. *Journal of Materials Research*, 4(6), 1354-1370. <https://doi.org/10.1557/JMR.1989.1354>
- [22] R.Chatterjee-Fischer (1989) Boriding and diffusion metallizing. *Surface modification technologies*, book, p.567-609.
- [23] I.Campos-Silva et al. (2010) Characterization of AISI 4140 borided steels. *Applied Surface Science*, 256(8), 2372-2379. <https://doi.org/10.1016/j.apsusc.2009.10.070>

## IZVOD

### JEDNOSTAVAN MODEL I INTEGRALNA METODA ZA SIMULACIJU RASTA BORIDNOG SLOJA FeB/Fe<sub>2</sub>B NA ČELIKU AISI H13

*Predviđanje kinetike rasta boridnog sloja zahteva razvoj matematičkog modela. U ovoj studiji predložena su dva modela difuzije (jednostavan model i model zasnovan na integralnoj metodi) za istraživanje kinetike borenja AISI H13 čelika sa bočnim pakovanjem. Ova dva modela difuzije nisu uzela u obzir efekat vremena inkubacije borida ukupnog sloja borida (FeB + Fe<sub>2</sub>B). Koeficijenti difuzije bora u slojevima FeB i Fe<sub>2</sub>B procenjeni su primenom predloženog modela zasnovanog na integralnoj metodi. Pored toga, određene su konstante brzine rasta i izračunata je debljina sloja nakon pronalaženja potrebnih parametara. Dobijeni rezultati su upoređeni sa eksperimentalnim rezultatima preuzetim iz rada Naita Abdelaha et al. [4] i uočen je dobar dogovor. Konačno, povećanje mase je izračunato za obe faze, pokazujući da se FeB povećava više u poređenju sa Fe<sub>2</sub>B tokom vremena.*

**Ključne reči:** model difuzije, simulacija, boronizacija, FeB, Fe<sub>2</sub>B, integralna metoda, debljina sloja

*Naučni rad*

*Rad primljen: 29. 08. 2023.*

*Rad korigovan: 22. 09. 2023.*

*Rad prihvaćen: 23.09.2023.*

*Rad je dostupan na sajtu: [www.idk.org.rs/casopis](http://www.idk.org.rs/casopis)*